PERGAMON

International Journal of Multiphase Flow 28 (2002) 997–1019

International Journal of Multiphase Flow

www.elsevier.com/locate/ijmulflow

Modeling the outcome of drop–drop collisions in Diesel sprays

Scott L. Post [1], John Abraham [*]

School of Mechanical Engineering, Purdue University, West Lafayette, IN 47907, USA

Received 12 July 2001; received in revised form 13 December 2001

Abstract

The sub-models for collisions and coalescence are important components of the spray model in multi-dimensional computations of Diesel sprays. These models influence the computed drop sizes, which affect the overall characteristics of the spray. Typically, the droplet interaction model is separated into two parts: first, calculating the collision rate between particles, and second, calculating the probability of coalescence once a collision has occurred. While the collision frequency may be estimated from kinetic theory considerations, a criterion has to be specified to determine the outcome of the collisions. The outcome may be bouncing, coalescence, stretching separation, or reflexive separation. The coalescence efficiency is defined as the probability that two drops will permanently merge into one drop, given that a collision between the two drops has occurred. Current approaches to modeling the coalescence efficiency are based on experimental observations of binary water drop collisions under atmospheric conditions. However, in the last decade experimental evidence has become available that suggests that the collision behavior of hydrocarbon drops may differ significantly from that of water drops. More recent experiments suggest that the effects of ambient pressure may also be significant. This paper presents a comparison of the computed outcome of drop collisions in a Diesel spray to that of recently published experimental observations. Possible ways to employ the recent findings in multidimensional spray models are discussed. Results of a model modified to reflect this new information is presented and compared with the original model. Limitations of the new model are discussed.

Keywords: Drops; Coalescence; Bounce; Sprays

1. Introduction

The modeling of liquid drop collisions and coalescence is important in modeling of Diesel sprays because collisions in a dense spray may have a significant impact on the mean drop size of

[*] Corresponding author. Tel.: +1-765-494-1505; fax: +1-765-494-0530.
E-mail address: jabraham@ecn.purdue.edu (J. Abraham).
[1] Department of Mechanical Engineering, Michigan Technological University, Houghton, MI 49931, USA

0301-9322/02/$ - see front matter
PII: S0301-9322(02)00007-1

the spray (O'Rourke and Bracco, 1980) and also on the dispersion and velocities of the drops (Gavaises et al., 1996). Since the droplet lifetime is approximately proportional to the square of the droplet diameter, the distance a droplet travels in a combustion chamber will have a strong dependence on the droplet size. In many diesel engine applications it is often undesirable for the spray droplets to travel far enough to impinge on the cylinder walls. Modeling of the droplet collision rate and coalescence efficiency is important in multidimensional computations to predict the penetration of the liquid drops (Aneja and Abraham, 1998). Droplet collisions may be especially important in the dense spray region where the droplet number density is the highest. The droplet interaction models that are commonly used (O'Rourke and Bracco, 1980; Gavaises et al., 1996) are based upon experimental observations of the behavior of water droplets. Recent experimental evidence (Jiang et al., 1992; Qian and Law, 1997) suggests that the collision behavior of hydrocarbon drops at elevated pressures can be significantly different than that of water drops at atmospheric pressure. These results will be reviewed in the next section. The impact of the difference in behavior between hydrocarbon and water drops on computed spray characteristics will also be discussed.

2. Experimental observations reported in literature

Until recently, most experimental studies on coalescence in binary drop collisions focused on water drops under atmospheric conditions due to meteorological interests. These studies include that of Brazier-Smith et al. (1972), whose results are often used in spray models, as well as the work of Ashgriz and Poo (1990) and others in the context of meteorology, as reviewed by Orme (1997). It is found that the outcomes of collisions can be described well by three non-dimensional parameters: the Weber number, We, the impact parameter, B, and the drop size ratio, γ.

$$We = \rho|v_1 - v_2|^2(r_1 + r_2)/\sigma \tag{1}$$

where ρ and σ are the density and surface tension of the liquid phase and v_1 and v_2 are the velocities of the smaller and larger drops, respectively, and r_1 and r_2 are the radii of the smaller and larger drops, respectively.

$$B = b/(r_1 + r_2) \tag{2}$$

where b is calculated by taking the distance from the center of one drop to the relative velocity vector placed on the center of the other drop. This is illustrated in Fig. 1. It can also be seen that $B = \sin\theta$, where θ is the angle between the line of centers of the drops at the moment of impact and the relative velocity vector. When $B = 0$ the collision is directly head-on, and when $B = 1$, the drops just barely graze each other. Drop size ratio can be defined in one of two ways.

$$\gamma = r_2/r_1 \tag{3}$$

$$\Delta = r_1/r_2 = 1/\gamma \tag{4}$$

where $r_2 > r_1$. The definition for Δ is often used in order to obtain a parameter, like B, that varies between 0 and 1.

Only recently have quantitative experimental results with hydrocarbon drops been published (Jiang et al., 1992; Qian and Law, 1997; Estrade et al., 1999). These three works are summarized

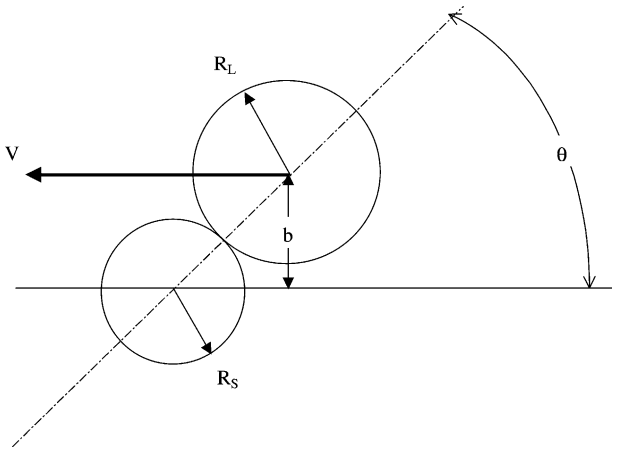

Fig. 1. Diagram illustrating the definition of impact parameter: $B = \mathrm{b}/(R_S + R_L)$.

in Table 1, along with the often cited results from Brazier-Smith et al. (1972), for comparison. Law and co-workers (1992, 1997) find that there are five distinct possible outcomes for a binary drop collision:

1. slow coalescence,
2. bounce,
3. coalescence,
4. reflexive separation,
5. stretching separation.

These regimes are shown in Fig. 2 on a *We–B* map. They can be described as follows: as the two drops approach each other, the air between them becomes trapped and the pressure can rise in the gap between the drops. If the drops are travelling slowly enough then the air has time to exit before the drops touch, so that slow coalescence can occur. However, if the drops' relative velocity

Table 1
Summary of important measurements of collision outcomes for drops

Author and year	Liquid fuel	Ambient gas	Weber number	Drop size (μm)	Ambient pressure (bar)	Drop relative velocity (m/s)	Drop size ratios
Estrade et al. (1999)	Ethanol	Air	5–200	80–300	1.0	3.0–12.0	1 and 2
Qian and Law (1997)	Tetradecane and water	Nitrogen	0.2–80	200–400	0.6–2.4	0.4–5.0	1
Jiang et al. (1992)	Water and Normal alkanes	Air	0–60	~150	1.0	0.4–4.0	1
Brazier-Smith et al. (1972)	Water	Air	0–80	150–750	1.0	0.3–3.0	1–2.5

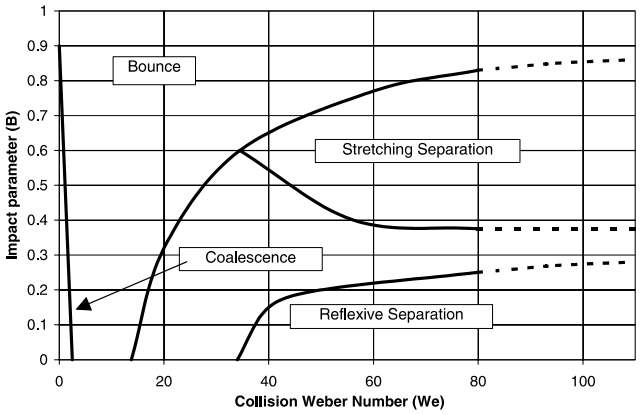

Fig. 2. Collisions outcome map for tetradecane drops in nitrogen environment. $T_a = 300$ K, $P_a = 1$ bar (Qian and Law, 1997).

is higher, there is not enough time for the gas to escape, and the pressure forces that arise will push the drops apart so they do not actually touch. This is referred to as bounce. The phenomenon of droplet bounce is not observed in water drops for head-on collisions at atmospheric pressure. At even higher drop velocities, the gas film that is formed between the drops can actually be absorbed into the liquid, so that coalescence can occur. At high Weber numbers, the drops have excess kinetic energy, and this can lead to separation of the drops from the temporarily coalesced drop. At high impact parameters, the drops tend to stretch apart, while for near-head-on collisions the drops can oscillate and undergo a reflexive separation. It has already been pointed out that water drops behave differently than hydrocarbon drops. In addition, the work of Qian and Law (1997) also shows that there are significant changes in the bouncing characteristics of drops from 0.6 to 2.4 atm. Fig. 3 shows their map of collision regimes at the higher pressure of 2.4 atm. The slow coalescence regime becomes undetectable as the high pressure makes it difficult for the drops to push away the ambient air without losing their kinetic energy. In order to quantitatively assess the

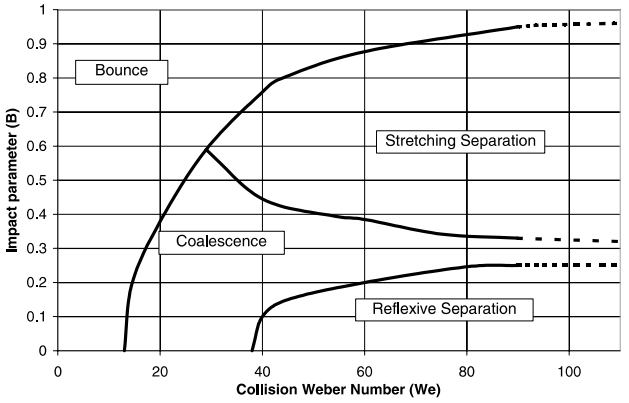

Fig. 3. Collisions outcome map for tetradecane drops in nitorgen environment. $T_a = 300$ K, $P_a = 2.4$ bar (Qian and Law, 1997).

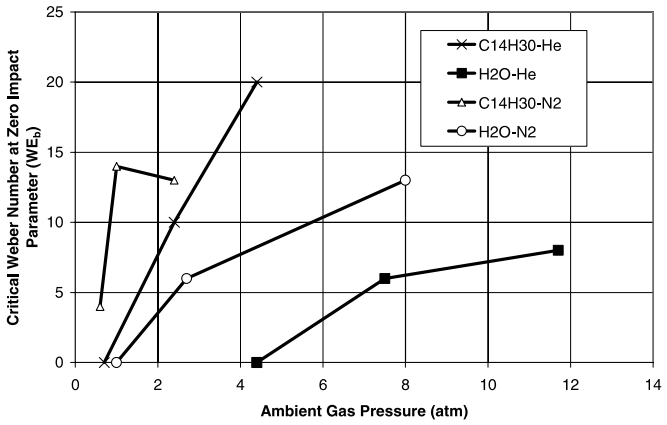

Fig. 4. Dependence of observed bouncing of drops on ambient gas pressure.

effect of the ambient pressure on the collision outcomes, we can define a critical Weber number, We_b, as the boundary between bounce and coalescence for an impact parameter of 0. Fig. 4 shows how the experimentally measured value of We_b varies for all of the gas–liquid systems that Qian and Law (1997) considered as a function of ambient pressure. It is obvious that We_b increases with ambient pressure, which implies that bounce is more important at higher ambient pressures. Furthermore, Qian and Law (1997) found that when vapor of a hydrocarbon species is added to the ambient, hydrocarbon drops are less likely to bounce and more likely to coalesce, and this effect becomes more significant as the ambient vapor content is increased. In this paper, we include the effects of pressure on bounce through a correlation derived from the experimental data. This will be discussed in a later section.

The work of Law and co-workers was the first quantitative work on hydrocarbon drops. Estrade et al. (1999) also made measurements for ethanol drops of equal size and size ratio of two (i.e. $\gamma = 1$ and 2). They also found that once separation, or fragmentation, occurs at a given impact parameter the number of satellite drops, or residues, increases as the Weber number is increased. Menchaca-Rocha et al. (1997) also made observations for mercury drops rolling on a glass surface. Unlike other works, they were able to measure the number, size, and velocity of the drops after a separation. However, their work may not be quantitatively comparable to other works in the literature, since the mercury drops also roll across the glass surface, as well as translate through space.

There are several limitations of the body of experimental works available in the literature, from the point of view of application to Diesel sprays. As Menchaca-Rocha et al. (1997) point out, any out-of-plane motion of the drops will not be captured with cameras, and interactions between the induced flow field of drops with the drop behind them is possible due to the small spacing between drops. Also, the experiments are typically limited to drop sizes of 100 μm and greater, Weber numbers below 100, and drop size ratios below 3, whereas in typical Diesel spray computations the drops are O(1 μm), Weber numbers can be O(1000), and drop size ratios O(10). As a result, the criteria we employ to determine outcomes of collisions have not been assessed for accuracy under Diesel spray conditions. The number of satellite drops formed, as well as their sizes and velocities, is not recorded. Furthermore, the effect of ambient gas properties such as density and viscosity is

not well understood, as well as the role of liquid viscosity or the Van der Waals forces of attraction. A submodel for shattering collisions that takes into account high *We* number effects has also been considered. This is also discussed later.

3. The contribution of this work

This work provides an assessment of the adequacy of the commonly used expressions for coalescence efficiency in multidimensional models for Diesel sprays. The characteristics of binary drop collisions under diesel conditions are discussed, and modifications to the current model are proposed. Implementation of these modifications is performed and the results are presented. The results are compared with those obtained from standard models that are currently employed. These recent expressions are, in part, based on experimental observations of the collisions of hydrocarbon droplets, as opposed to water droplets in earlier experiments. The need for further modifications is discussed. Differences in the computed structure of the spray in the dense spray regime and effects on mean drop sizes and liquid phase penetration are discussed.

4. The multidimensional model used for diesel computations

The model employed in this work is an axisymmetric version of a more general model for computing flows, sprays, and combustion in internal combustion engines (Magi, 1987, 1999). The model solves the unsteady, turbulent two-phase flow of liquid drops in gas. The gas phase is treated in an Eulerian fashion. The general ensemble-averaged conservation equations of mass, momentum, energy and species for unsteady compressible flows are solved with sub-models for turbulence and heat and momentum fluxes at the walls. Turbulence is modeled using the k–ε model and the heat and momentum fluxes at the wall with wall functions.

The liquid phase is treated in a Lagrangian frame of reference using the discrete parcel approach (O'Rourke and Bracco, 1980). Since there are too many drops in a typical Diesel spray to track individually, the drops are collected into parcels. Each parcel contains a number of drops that have identical size, velocity, and temperature. The parcels of drops are tracked in space and time. The drops that compose the parcel are assumed to be uniformly distributed throughout the Eulerian gas cell in which the parcel is located. The liquid and the gas momentum are coupled through the drag and pressure forces. Atomization is modeled by a line source of drops (Chatwani and Bracco, 1985). The initial angle of the spray, the size of the injected drops and the steady intact core length are derived from Taylor's theory of the rate of growth of perturbations on planar liquid surfaces induced by gases flowing over it. The resulting expressions can be found in Refs. (Magi, 1987; Chatwani and Bracco, 1985).

Drop dispersion due to turbulence is modeled using the eddy-lifetime approach of Gosman and Ioannides (1981). A secondary drop break-up model is also used (Reitz and Diwaker, 1987). The vaporization rate is modeled by solving the quasi-steady equation for mass and energy conservation for individual drops (O'Rourke and Bracco, 1980). The expression for drop size is

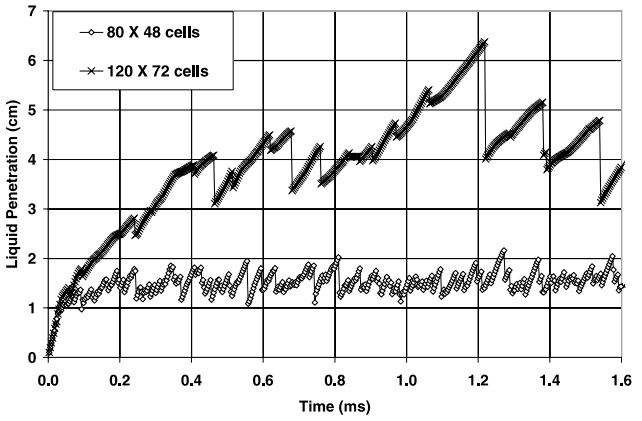

Fig. 5. Resolution dependence of computed spray penetration for a Diesel spray.

$$\bar{d}_{\text{drop}} = B_{\text{d}} \frac{2\pi\sigma}{\rho_{\text{a}} U_{\text{T}}^2} \lambda_{\text{m}}^* \tag{5}$$

Here B_{d} is a constant that depends on the nozzle geometry, U_{T} is the velocity of the fastest growing unstable wave, which is proportional to the injection velocity. Following Bracco (1985) and Chatwani and Bracco (1985), we have taken the value for the constant B_{d} to be 0.62. Following Chatwani and Bracco (1985), $U_{\text{T}} = 0.25 \times U_0$, where U_0 is the injection velocity of the spray, and λ_{m}^* is a function of the liquid viscosity parameter in Taylor's theory of drop formation (Bracco, 1985).

Collision and coalescence are modeled using the approach of O'Rourke and Bracco (1980). The collision frequency between drops is calculated based on the number density of drops and relative velocity between the drops. Unfortunately, this methodology leads to a dependence of the computed collision rate on the spatial grid resolution employed. This is illustrated in Fig. 5, where the same computation is performed on two different spatial grids. These sprays are computed for an injector orifice of 0.246 mm with an injection velocity of 460 m/s, and ambient conditions of 1000 K and 14.8 kg/m^3, which are representative of the conditions inside a Diesel engine. The instantaneous liquid penetration is defined as axial position of the parcel that has traveled the furthest from the orifice. This is discussed further in the work of Aneja and Abraham (1998). The outcome of a collision can either be coalescence or separation. The criterion for drop separation after collision is the Brazier-Smith model, which is discussed in detail in the next section.

5. Models for outcomes of collisions

5.1. Traditional approach to modeling collision outcome

Once a collision has occurred, the outcome of the collision must be determined. Collisions are calculated by a statistical, rather than a deterministic, approach. Either all of the drops in the parcel collide, or none of them collide. It is also assumed that the drops are uniformly distributed

in the computational cell. The criterion for separation is that the rotational energy of the coalesced drop exceeds the surface energy required to reform the original drops from the coalesced pair. The coalescence efficiency, E_{coal} is defined as the probability of coalescence once a collision has occurred. O'Rourke and Bracco (1980) employ, based on Brazier-Smith et al.'s (1972) derivation

$$E_{coal} = \min(1.0, 2.4f(\gamma)/We) \tag{6}$$

where the complex function $f(\gamma)$ is approximated by a polynomial for simplicity

$$f(\gamma) = \gamma^3 - 2.4\gamma^2 + 2.7\gamma \tag{7}$$

The Brazier-Smith model is a relatively simple energy balance model. Assuming no dissipation, they calculated the rotational energy of the drop pair as a function of the impact parameter and the density of the liquid and the relative impact velocity. The increase in surface energy that would be required to reform the original drops from the temporarily coalesced drop pair is calculated, which is a function of the drop size and the drop size ratio. The resulting expression, Eq. (6), can be formulated solely in terms of the Weber number, impact parameter, and drop size ratio. The strong drop size ratio effect arises because the Weber number is based on the size of the smaller drop. For a constant Weber number and smaller drop size, increasing γ increases the size of the larger drop. The larger the size of the larger of the two drops, the more easily it can absorb the smaller drop.

This criterion is shown on a three-dimensional collision outcome map in Fig. 6. The surface shown represents the boundary between permanent coalescence and stretching separation. If a point lies above the surface, the excess kinetic energy of the temporarily coalesced drop pair is too great for it to remain stable, and it splits into the original two drops. O'Rourke and Bracco (1980) term this a grazing collision. If the collision is a grazing collision, an appropriate amount of kinetic energy is dissipated in the process, which is determined by the impact parameter. Satellite drop formation is not included in the model of O'Rourke and Bracco (1980).

The definition of coalescence efficiency implies that off-center collisions are more likely than head-on collisions. Brazier-Smith et al. (1972) define the coalescence efficiency to be equal to the

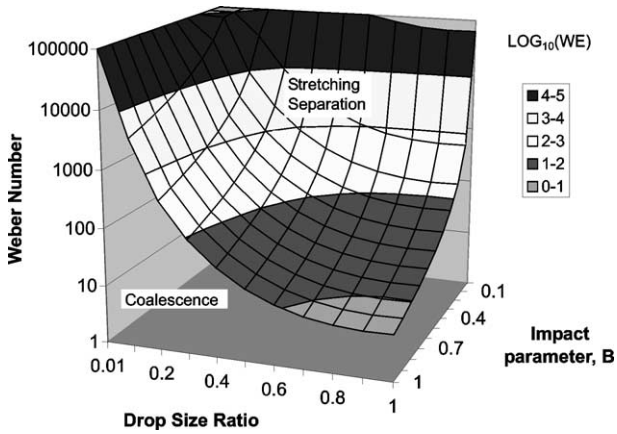

Fig. 6. Three-dimensional map identifying stretching separation and coalescence regimes (Brazier-Smith et al., 1972).

square of the impact parameter. Since the collision events in Diesel spray computations are stochastic rather than deterministic, the impact parameter for each collision is not calculated deterministically. O'Rourke and Bracco choose a random number from a uniform distribution in the range [0,1]. If the random number is less than the coalescence efficiency then coalescence occurs, otherwise the collision is considered a grazing collision. The implication of this definition is that in a turbulent spray, all values of the square of the impact parameter are equally likely in binary collisions, which results in a distribution for the impact parameter, B, that is biased towards values closer to 1. The impact parameter is chosen in this way since off-center collisions are more likely than near-center collisions due to the greater cross-sectional area associated with large values of B. This is true because the differential cross-sectional area for collision associated with a particular value of B is $2\pi B\,\mathrm{d}B$. After normalization, this yields a pdf for B

$$\mathrm{pdf}(B) = 2B \tag{8}$$

for $0 \leqslant B \leqslant 1$. Fig. 7 shows the pdf for B, along with the results of a discrete simulation that verify this pdf. In the simulation a large number of drops are allowed to pass through a window at a distance, H, away from an equal sized drop at the coordinate axes origin. The window has a characteristic dimension five times greater than the drop size. The initial position of the drop and the three components of its velocity are chosen from uniform random distributions. The drops are assumed to travel in a straight line and the impact parameter is calculated for all drops that collide with the drop at rest in the center of the domain. The results are found to be insensitive to the size of the window and its position, provided both are significantly larger than the drop size.

Similarly, following the explanation of Gavaises et al. (1996), an equivalent method is to choose a random number, yy, in the range (0,1), and then calculate

$$b = \sqrt{(yy)(r_1 + r_2)} \tag{9}$$

$$b_{\mathrm{cr}}^2 = (r_2 + r_1)^2 \min(1.0, 2.4 f(\gamma)/We_{\mathrm{d}}) \tag{10}$$

If $b < b_{\mathrm{cr}}$, where b_{cr} is the critical impact parameter, then the result of every collision is coalescence. If $b \geqslant b_{\mathrm{cr}}$, then every collision is a grazing collision, but the drops' velocities do change.

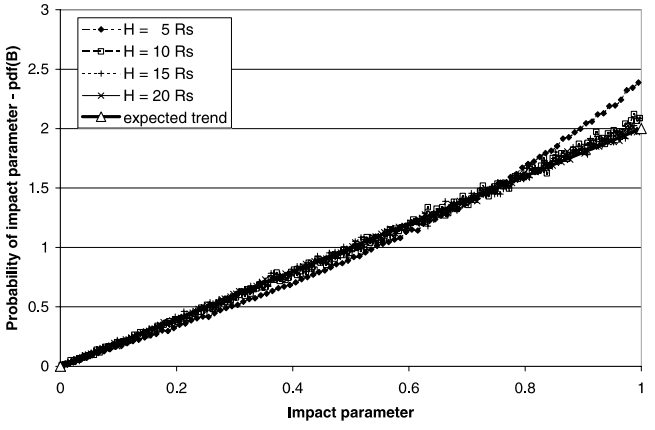

Fig. 7. Results of 25×10^6 discrete simulations with droplets released a distance H from target drop and with random initial orientation and velocity.

Here the critical value of b, rather than E_{coal} has been calculated directly, and Eq. (10) is equivalent to Eq. (6) using the definition of $E_{coal} = B^2 = (b/(r_1 + r_2))^2$.

If coalescence does occur, then the number of coalescences, n, is determined by finding the value of n for which

$$\sum_{k=0}^{n-1} P_k \leqslant xx < \sum_{k=0}^{n} P_k \tag{11}$$

For each of the larger drops, which is also called a collector drop, n droplets are subtracted from their associated parcel, and the properties of the collector drops are appropriately modified using the conservation equations. If there are not enough droplets to have n coalescences with each collector, then n is recomputed so that all N_2 droplets coalesce, and the parcel associated with the droplets is removed from the calculation.

If a grazing collision is the outcome of the collision, then only one collision is calculated for each drop. Grazing collisions are calculated between N pairs of drops, where N is the minimum of N_1 and N_2 The N collectors and droplets are then returned to their parcels in such a way that mass, momentum, and energy are conserved. The velocity of each particle after a grazing collision is given by

$$U_1^{new} = \frac{U_1 r_1^3 + U_2 r_2^3 + r_2^3 (U_1 - U_2) zz}{r_1^3 + r_2^3} \tag{12}$$

where

$$zz = \frac{B - B_{cr}}{(r_1 + r_2) - B_{cr}} \tag{13}$$

5.2. Reflexive separation model

The criterion proposed by Ashgriz and Poo (1990) for reflexive separation is given by

$$We > 3[7(1 + \Delta^3)^{2/3} - 4(1 + \Delta^2)] \frac{\Delta(1 + \Delta^3)^2}{\Delta^6 \eta_1 + \eta_2} \tag{14}$$

where the parameters $\eta_1 = 2(1 - \xi)^2 (1 - \xi^2)^{1/2} - 1$ and $\eta_2 = 2(\Delta - \xi)^2 (\Delta^2 - \xi^2)^{1/2} - \Delta^3$, and $\xi = (1/2)B(1 + \Delta)$. η_1 and η_2 are the fractions of the drops' kinetic energy that participates in the reflexive separation process. This is based on a balance between kinetic energy and surface energy. They assume that after the contact the two drops form a flattened disc which quickly changes shape to a cylinder which stretches out under the force of the internal flow of the fluid moving in opposite directions. It would then seem to be logical to use a simple balance between this effective reflexive energy and the nominal surface energy. However, once the cylinder has stretched far enough for a thin ligament to form, the surface energy can then be reduced by forming two drops, so that separation can occur even if the reflexive energy is less than the surface energy. Based on Rayleigh's linear theory, they calculate that if the effective reflexive energy is more than 75% of the nominal surface energy, then reflexive separation will occur. This criterion shows good agreement

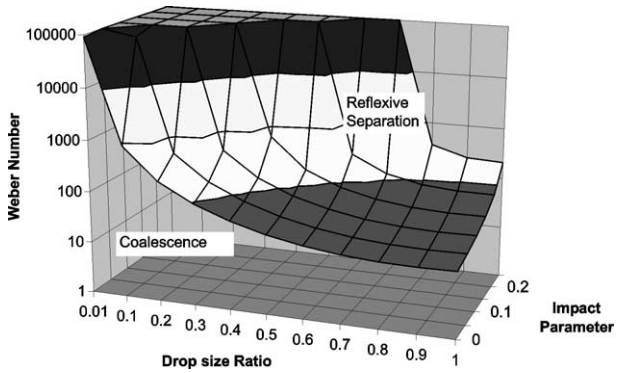

Fig. 8. Reflexive separation and coalescence regimes from criteria of Ashgriz and Poo (1990).

with their experimental results. Their criterion is shown in Fig. 8. It can be seen here that as for the Brazier-Smith model, coalescence becomes more likely for unequal sized drops.

Tennison et al. (1998) performed computations where Ashgriz and Poo's (1990) reflexive separation criterion is included. They attempted to model kinetic energy dissipation for reflexive separation. They also attempted to include bounce, but did not include the effects of impact parameter or drop size ratio on bounce.

5.3. Bounce model

Estrade et al. (1999) provide the first expression to predict bouncing. Based on their experimental observations, they assume that the drops deform into semi-spherical shapes as they approach each other. If the deformation of the drops as they approach each other produces an increase in surface energy that is greater than the initial kinetic energy of the pair, then the drops will bounce. They neglect viscous forces and dissipation. The criterion for coalescence to occur is given by

$$We > \frac{\Delta(1+\Delta^2)(4\phi' - 12)}{\chi_1(\cos(\arcsin B))^2} \tag{15}$$

where ϕ' is the shape factor,

$$\chi_1 = 1 - \frac{1}{4}(2-\tau)^2(1+\tau) \quad \text{if } \tau > 1.0$$

or

$$\chi_1 = \frac{1}{4}\tau^2(3-\tau) \quad \text{if } \tau \leqslant 1.0$$

and $\tau = (1-B)(1+\Delta)$. The shape factor ϕ', which is a measure of the deformation of the drops from their initial spherical shape, is given a value of 3.351 by Estrade et al. (1999). This is shown on a three-dimensional map in Fig. 9. In this figure, where the surface represents the boundary between bouncing separation and coalescence, any point below the surface leads to a bouncing

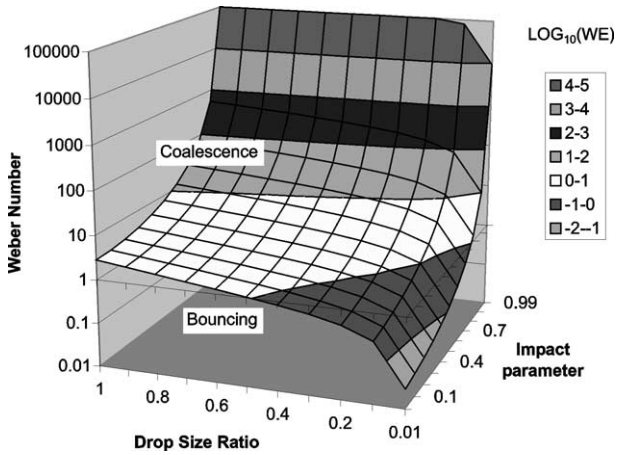

Fig. 9. Three-dimensional map identifying bouncing separation and coalescence from criteria of Estrade et al. (1999).

separation. There are two limitations to this criterion. First, the parameter ϕ' must be fit to experimental data. Second, interaction with the ambient fluid is neglected, so this model cannot reproduce Qian and Law's (1997) experimentally observed results of bounce becoming more prevalent at higher ambient pressures, and less prevalent as the vapor content of the ambient is increased.

5.4. Modeling the effect of pressure

It can be seen from Fig. 4 that the critical Weber number for bouncing varies with ambient gas pressure, or density since the temperature is held constant, with a less than linear dependence. For drops in a Diesel spray the Reynolds numbers will be O(100). For this range of Re, the drag coefficient can be expressed as

$$C_D = \frac{24}{Re}\left(1 + \frac{Re^{2/3}}{6}\right) \tag{16}$$

For high Re, then $C_D \sim Re^{-1/3}$. The drag force on a drop is

$$F_D = C_D \frac{\pi}{8}\rho_a V^2 d^2 \tag{17}$$

Hence, the drag force, F_D, is proportional to the ambient density to the 2/3 power. If we then assume that the deformation energy of the drops in the bouncing regime will be proportional to the drag force, then the critical shape factor in Eq. (15) for bouncing should increase with the ambient gas density to the 2/3 power. This would lead to an approximate dependence of Weber number on ambient density to the 2/3 power, which is in qualitative agreement with the experiment trends shown in Fig. 4. Therefore, for modeling sprays in high-pressure environments, we have modified Eq. (15) such that

$$\phi' = \phi'_0(\rho_a/\rho_0)^{2/3} \tag{18}$$

where $\rho_0 = 1.16$ kg/m^3. For tetradecane, Jiang et al. (1992) found that at $B = 0$, $We_b = 14$ under atmospheric conditions. For a gas density of 14.8 kg/m^3, this dependence will lead to a critical Weber number $We_b = 52$ at $B = 0$.

5.5. Modeling shattering collisions

One possible outcome of drop–drop collisions is the break-up of the original drops into smaller drops. There are two possible ways that this could happen. One of the ways appears to be a surface-tension dominated phenomenon which has been referred to as "spattering" by Gunn (1965) and Park (1970) and the other is drop pulverization which is referred to as "shattering" by Park (1970). However, Georjon and Reitz (1999) refer to the surface-tension dominated phenomena as "shattering". To add to this terminology, Frohn and Roth (2000) use the term "splashing" to refer to what appears to be the surface-tension dominated phenomena. In this work, we will employ the term "shattering" to refer to the surface-tension dominated phenomena following the work of Georjon and Reitz (1999). Georjon and Reitz (1999) proposed a model for shattering collisions between drops. They assumed that after the drops collide they form a ligament, which stretches due to the inertia of the collision. One limitation of their work is that it is assumed all the satellite drops have the same size, whereas the experimental works (Jiang et al., 1992; Qian and Law, 1997) indicate that the satellite drops are usually much smaller than the parent drops. This could also be a function of impact parameter, which will influence the size of the ligament between the drops. The higher the value of the impact parameter, the smaller the volume of fluid interacting, and hence the smaller the size of the ligament. They derive the following equation, which governs how the size of the cylinder changes with time

$$\ddot{r} = \frac{9\sigma r_c^4}{16\rho R_0^6} - \frac{27\sigma r_c^7}{32\rho R_0^9} + 3\frac{\dot{r}^2}{r} \tag{19}$$

Here r_c is radius of the cylinder and R_0 is the radius of the spherical drop that would be formed if the two original drops coalesced. A severe limitation of this model is that it increases the computational time. However, this limitation can be dealt with by recognizing that shattering collisions will only be important at high Weber numbers. Taking Eq. (19) and non-dimensionalizing it using the transformations $r^* = r_c/R_o$ and $t^* = 0.5tU/R_o$, the equation can be re-written as:

$$\ddot{r}^* = \frac{9}{4We\sqrt[3]{1+\Delta^{-3}}} r^{*4} - \frac{27}{8We\sqrt[3]{1+\Delta^{-3}}} r^{*7} + 3\frac{\dot{r}^{*2}}{r^*} \tag{20}$$

with the boundary conditions: $r^*(0) = 1$ and $\dot{r}^*(0) = -0.75\ \alpha$, where α is a constant of O(1). Taking the limit of high We, we can eliminate the first two terms on the right-hand side of Eq. (20). The resulting equation has the analytical solution

$$r^* = \frac{1}{\sqrt{1.5\alpha t^* + 1}} \tag{21}$$

Combining this with the non-dimensional breakup time

$$t^* = 9.24\sqrt{We\sqrt[3]{1+\Delta^{-3}}}\, r^{*3/2} \tag{22}$$

and taking the highest order term yields the following expression for the size of the cylinder at breakup. Using a value of $\alpha = 0.44$, this yields the drop size formed due to shattering as

$$r^*_{\text{child}} = \frac{1.89}{\sqrt{2.81 We^{2/7}(1 + \Delta^{-3})^{2/21} + 1}} \tag{23}$$

It is worth noting that we have not included the effects of the ambient gas on initializing or enhancing the waves which breakup the cylinder. While Frohn and Roth (2000) find the onset of shattering collisions to be between $We = 1000$ and 1800, Willis and Orme (2000) have noted that shattering does not occur in a near-vacuum environment even for Weber numbers up to 3200. However, Gunn (1965) and Park (1970) have observed "spattering" to occur at $We<200$. Georjon and Reitz use their criterion when $We>100$.

5.6. A composite collision outcome model

A new coalescence model is now described which takes reflexive separation and bounce into account, as well as rotational separation. This composite model is formulated by first using Eq. (9) to calculate b, and then B, with the Weber number and drop size ratio known. Then Estrade et al.'s (1999) criterion, Eq. (15), is used to determine whether or not bouncing has occurred. If

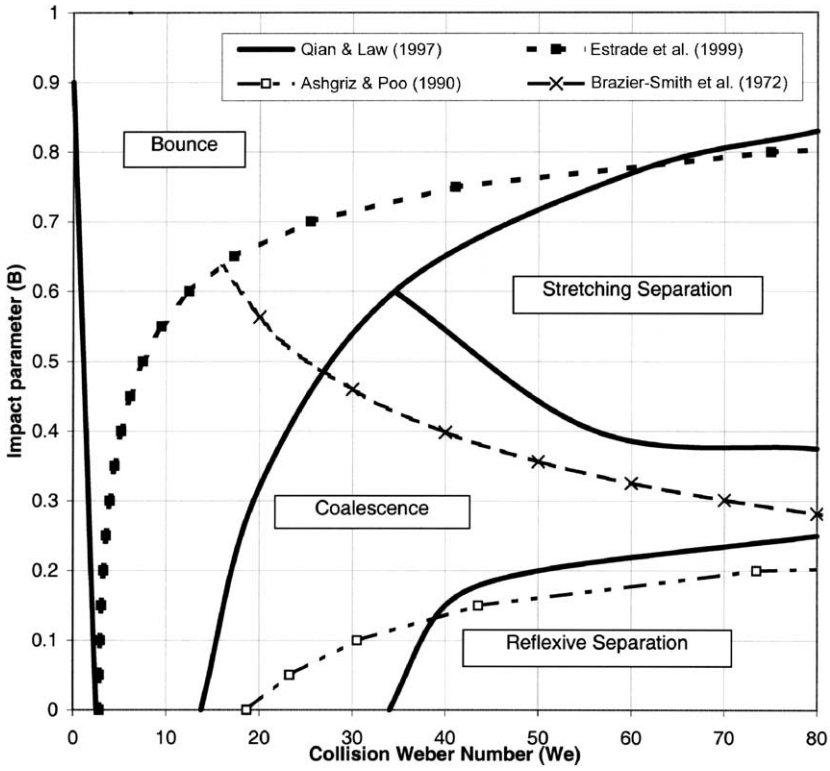

Fig. 10. Comparison of analytical and experimental collision regimes. $P_a = 1$ bar; equal size drops.

bounce has not occurred, then coalescence has occurred, at least temporarily. Then the criteria of Brazier-Smith et al. (1972), Eq. (10), and Ashgriz and Poo (1990), Eq. (14), are employed to determine whether a separation has occurred. Even though there are many expressions in the literature for stretching separation, e.g. Menchaca-Rocha et al. (1997), we have chosen to continue to use the Brazier-Smith criterion because it the fits experimental data as well as any of the other proposed criteria (Ashgriz and Poo, 1990; Menchaca-Rocha et al., 1997) and it is easy to employ computationally. O'Rourke and Bracco's (1980) original model for kinetic energy dissipation has not been modified in the case of reflexive separation or bouncing, i.e. no kinetic energy is dissipated. Also, as in the work of Tennison et al. (1998), we do not employ Jiang et al.'s (1992) corrections for liquid phase properties, since these are empirical in nature and also do not account for possible changes in the shapes of the curves with varying impact parameter or drop size ratio.

Fig. 10 presents a comparison of the new composite model discussed above with the experimental results of Qian and Law (1997) for equal size drops. While adding the models of Ashgriz and Poo (1990) and Estrade et al. (1999) provides better qualitative agreement than using only the Brazier-Smith et al. (1972) model, there are still significant quantitative differences.

6. Computational domain and conditions

There are two separate sets of computations reported here. In the first set, computations are reported in a 5 cm × 5 cm× 0.5 cm domain where parcels are uniformly distributed in the domain. We have employed several spatial resolutions in our computations. The resolution will be reported as $N_1 \times N_2 \times 1$, where N_1 is the number of cells axially and N_2 is the number of cells radially. There is one cell in the depth of the volume. A key assumption in the Lagrangian-drop-Eulerian-fluid model is that the parcels (and drops) are uniformly distributed in space. The domain and parcel distribution have been selected to approximate this. The initial mean velocities in the domain are zero, but initial values of k and ε are specified such that the mean turbulence intensity, $(2k/3)^{1/2}$, is 2200 cm/s and the turbulence length scale, $0.16432\, k^{3/2}/\varepsilon$, is 0.34 cm. As a result of the turbulence, the parcels will move and interact. The second set of computations reported is in the axisymmetric chamber shown in Fig. 11. Injection and chamber conditions are selected to approximately match those in the measurements of Siebers (1998), which is of

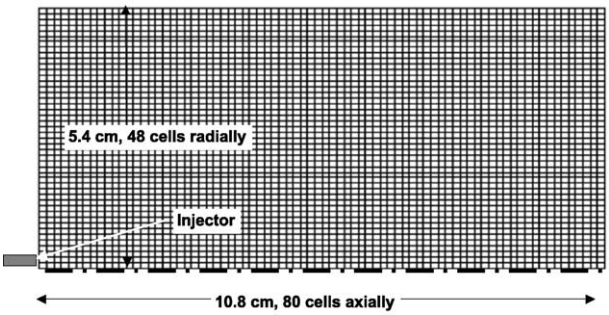

Fig. 11. Computational grid employed.

relevance to Diesel sprays. Parcels are injected at a rate of 5000 parcels/ms over the 2 ms duration of the injection event. The orifice diameter is 246 μm and the injection velocity is 460 m/s. The fuel is tetradecane, which has a density of 763 kg/m^3 and a surface tension of 0.022 J/m^2 at 300 K. The drops are injected along the centerline of the cylinder of radius 5.4 cm and length 10.8 cm. A uniform resolution of 80 cells axially and 48 cells radially is used, so that the cell size is of the order of 1 mm. Higher resolution computations are also presented. For the conditions corresponding to the experiments of Qian and Law (1997) with an ambient of nitrogen at 1.0 atm, the Sauter mean diameter (SMD) of the injected drops is 9.5 μm, and with the ambient at 2.4 atm, the SMD is 4.1 μm, while for the computations corresponding to Siebers' (1998) experiments, with an ambient density of 14.8 kg/m^3, the SMD is 0.84 μm. These drop sizes are obtained from Eq. (5). Unless mentioned otherwise, the ambient temperature for the spray computations is 1000 K.

7. Results and discussion

Fig. 12 shows the SMD of the drops in the "box" geometry as a function of time obtained by employing the Brazier-Smith et al. (1972) model for coalescence efficiency. Results are presented for four resolutions. It may be seen that the results do not change significantly for resolutions greater than $40 \times 40 \times 1$. At 100 ms after start of computation, the SMD has increased from an initial value of 2 μm to about 2.85 μm, an increase of greater than 40%. Fig. 13 shows the results when the composite coalescence model proposed here is employed and compares them with results from the model of Brazier-Smith et al. (1972). Results are presented for the same two resolutions where convergence is achieved. At 100 ms after start of computation, the SMD has increased to about 2.17 μm with the composite model, an increase of less than 10%, whereas it has increased to about 2.85 μm with the Brazier-Smith et al. (1972) model, an increase of over 40%. Hence, the composite model predicts a noticeably lower coalescence efficiency relative to the Brazier-Smith et al. (1972) model. The primary difference between the two models is the inclusion of the sub-model for bounce, which reduces the tendency to coalesce.

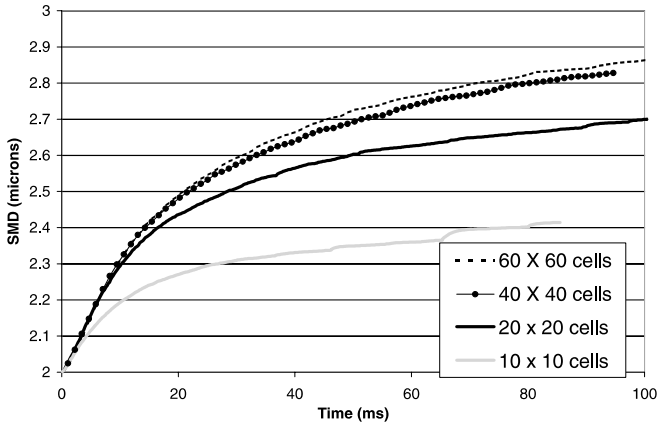

Fig. 12. Computed SMD for 10,000 parcels uniformly distributed throughout a $5 \times 5 \times 0.5$ cm domain at 300 K, 1.16 kg/m^3. 1000 drops per parcel. Brazier-Smith et al. (1972) coalescence model employed.

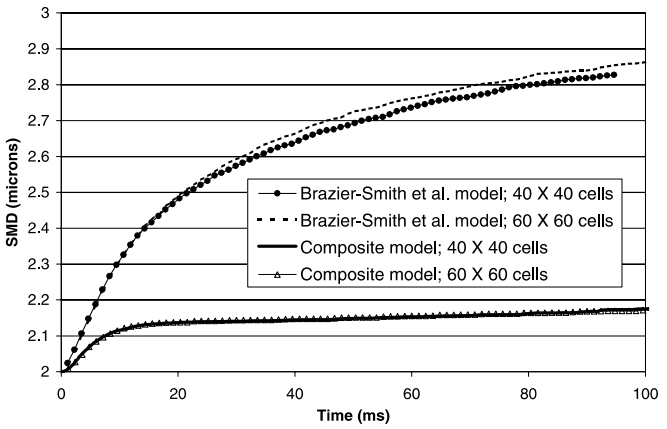

Fig. 13. Computed SMD for 10,000 parcels uniformly distributed throughout a $5 \times 5 \times 0.5$ cm domain at 300 K, 1.16 kg/m^3. 1000 drops per parcel. Brazier-Smith et al. (1972) and composite models are compared.

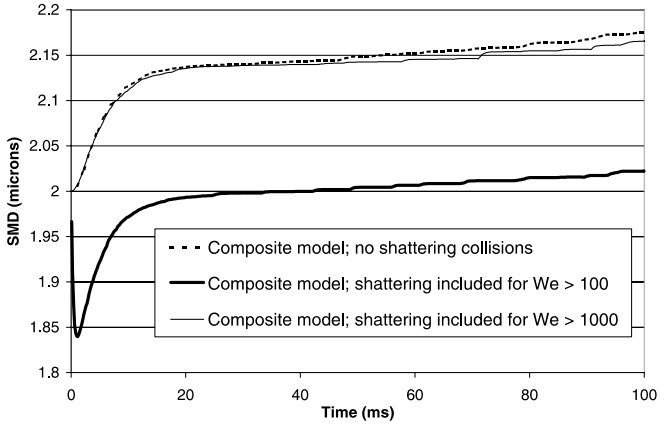

Fig. 14. Computed SMD for 10,000 parcels uniformly distributed throughout a $5 \times 5 \times 0.5$ cm domain at 300 K, 1.16 kg/m^3. 1000 drops per parcel. Grid resolution is 40×40 cells.

We have also examined how the model for shattering collisions affects the computed outcomes. Fig. 14 shows results with the composite model when shattering collisions are not included and compares them to computations when we have allowed shattering to occur for collisions with $We > 100$ in one case and for $We > 1000$ for another case. The choice of these cut-offs for We are somewhat arbitrary and are meant to give insight into how shattering collisions might affect computed results. In the computations with shattering, shattering is only allowed to occur after a rotational or a reflexive separation has been predicted by the composite model. Shattering does not occur after a bouncing separating, since the drops do not actually touch during bouncing and the disruption of the drops' surfaces necessary for shattering does not occur. As can be seen in Fig. 14, there is negligible difference in results when shattering is allowed for $We > 1000$. This indicates that most of the collisions in this problem are at We lower than 1000. When shattering is

predicted for $We > 100$ there is a larger difference initially as the drop size reduces by about 10%. The differences arise in the early stages of computation when the *We* numbers are larger and shattering is more dominant. As the initial turbulence in the box decays, the We of the collisions becomes lower and the drops stop shattering and coalesce. To assess the impact of the coalescence model on computed Diesel sprays, computations were carried out in the axisymmetric chamber described in the previous section.

Results of *spray* computations with the new composite coalescence model will now be presented. Fig. 15 shows the frequency of occurrence of collision outcome with the Brazier-Smith et al. (1972) model, the composite model with gas density effects included and the composite model with gas density and shattering effects included. The results shown are for a spray with an injection velocity of 460 m/s and with the chamber at 1000 K and 14.8 kg/m^3. For the case shown, when the Brazier-Smith et al. (1972) model is employed, coalescence occurs in about 53% of collisions and stretching separation in 47% of the collisions. When the composite model is employed, with gas density effects included, but not the model for shattering collisions, coalescence occurs in about 5% of the collisions, stretching separation in about 16% of the collisions, bounce in about 78% of the collisions and reflexive separation in about 1% of the collisions. The significant difference relative to the Brazier-Smith et al. (1972) model is the dominant effect of bounce. When the model for shattering is included, shattering occurs in about 6% of the collisions. For comparison, results with the Brazier-Smith et al. (1972) model are also shown. Fig. 16 shows the computed penetration and Fig. 17 the SMD. Results where the model does not include density effects and where it includes such effects are shown. See Section 5.4 for a discussion of the model. It can be seen that at a resolution of 80×48, corresponding to grid dimensions of about 1.2 mm,

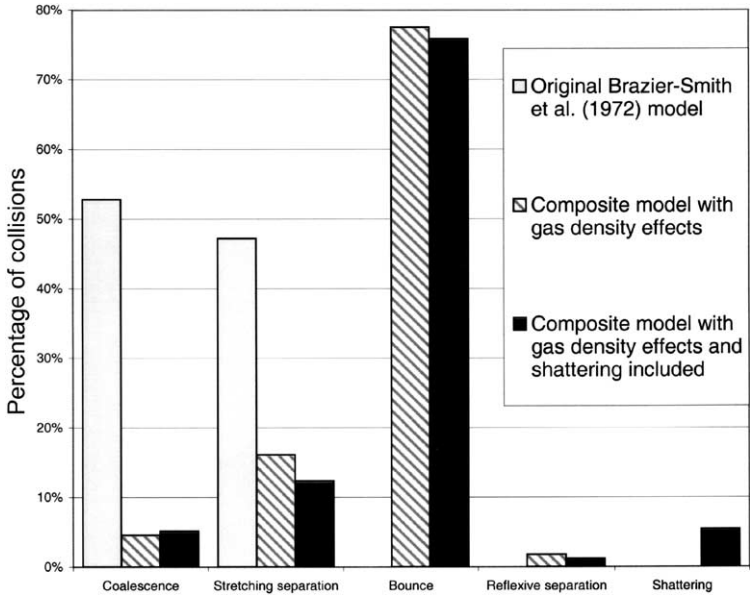

Fig. 15. Frequency of collision outcomes with different models for a spray computation.

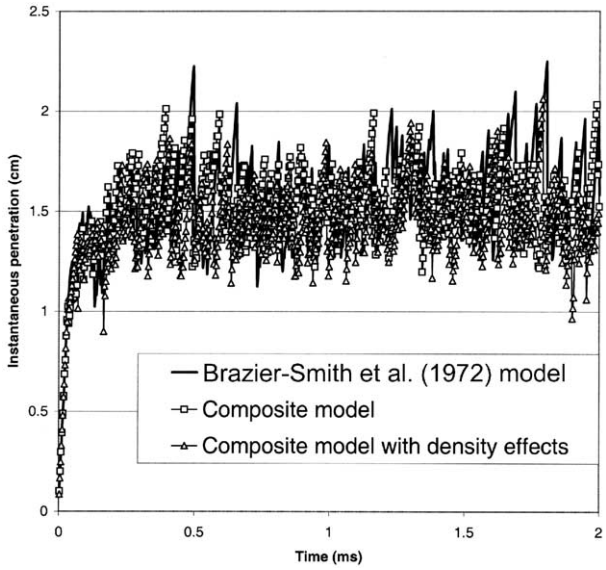

Fig. 16. Liquid penetration for resolution of 80×48 cells. $U_0 = 463$ m/s.

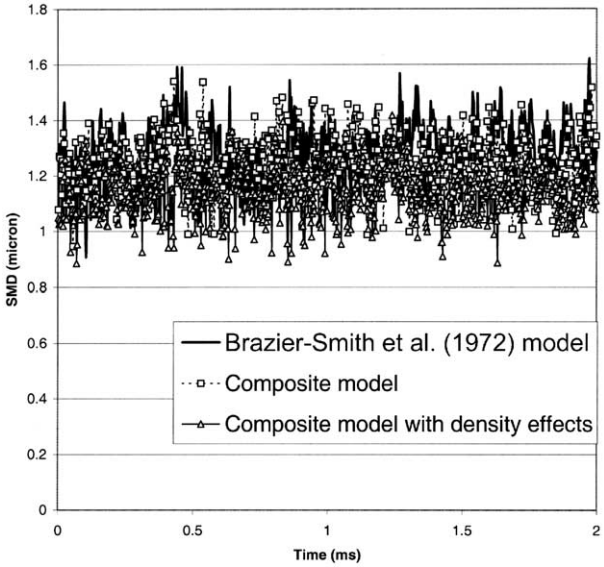

Fig. 17. Instantaneous SMD of drops in chamber for resolution of 80×48 cells.

which is typical of engine computations, there is not much difference in the computed penetration or SMD of the spray. At Weber numbers that are greater than about 30, the inclusion of Estrade et al.'s (1999) original bounce model is largely inconsequential. This can be seen in Fig. 10, where for equally sized drops, above a Weber number of 30 all of the predicted bounces would have been

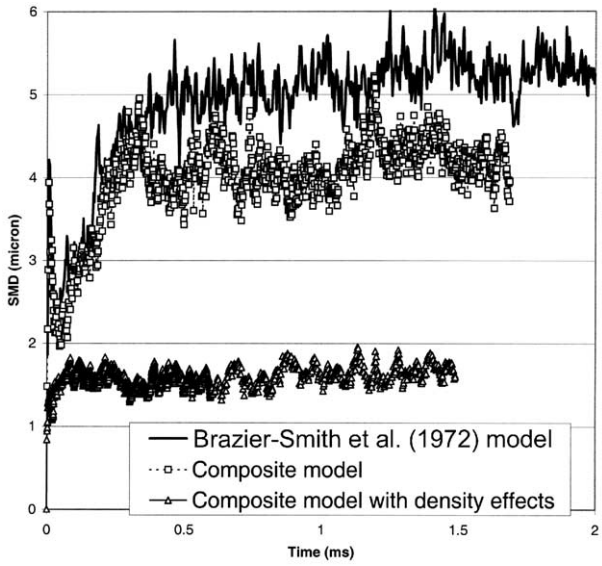

Fig. 18. Computed SMD for highest resolution of 220×110 cells. 1000 K, 14.8 kg/m^3.

predicted as separations with the Brazier-Smith et al. (1972) model. Including the effects of the higher chamber gas density does not have a significant effect at this resolution.

However, at higher resolutions, significant differences are seen in the computed SMD, as shown in Fig. 18. Here a grid resolution of 220×110 is employed. At the highest resolution of 220×110 cells, the cell size is 0.49 mm, which is twice the orifice diameter. The difference between the three coalescence models is accentuated due to the increase in the computed apparent collision rate as the grid size is decreased. At the lower resolutions, differences between models are overwhelmed by numerical errors. The challenge here is that the grid resolutions that are typically employed in spray computations are unable to capture the physics with adequate accuracy. Hence, there are

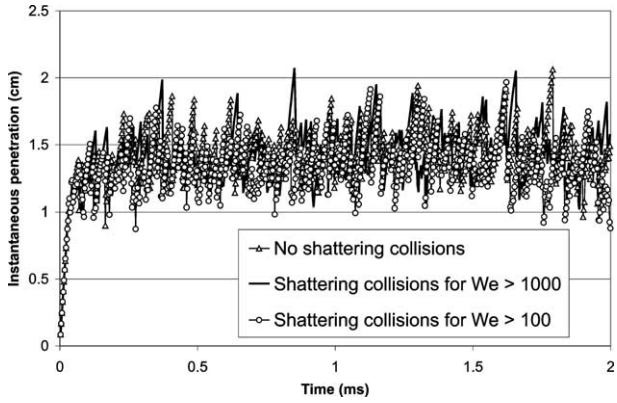

Fig. 19. Liquid penetration fro a resolution of 80×48 cells. In all cases the composite model with density effects is used.

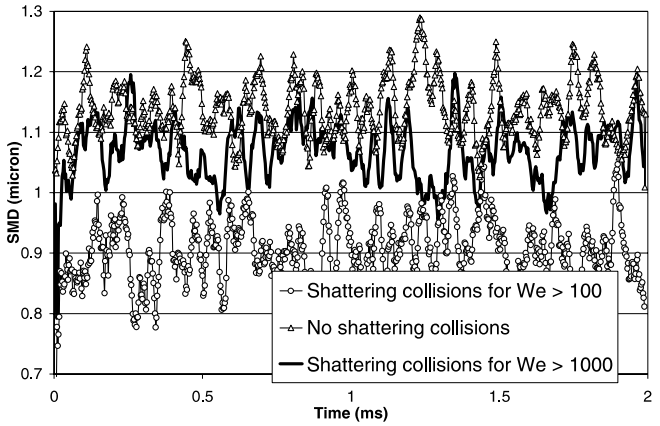

Fig. 20. Instantaneous SMD of drops in chamber for resolution of 80×48 cells. In all cases composite model with density effects is used.

noticeable and significant differences in outcomes between the different models. Nevertheless, it is encouraging that the qualitative changes observed in Fig. 18 are in the right direction.

For the lowest resolution used of 80×48 cells, including the effects of shattering collisions decreases the mean liquid penetration by about 8%, as can be seen from Fig. 19. In the model of Georjon and Reitz (1999) shattering collisions occur for Weber numbers greater than about 100. There is no consensus in the literature about the *We* number above which shattering becomes dominant. We have also performed a computation where we have allowed shattering collisions only for $We > 1000$. Results are shown in Fig. 19. For these computations, roughly one-third of the collisions occur at Weber numbers less than 100, one-third for $100 < We < 1000$, and one-third at $We > 1000$. Fig. 20 shows the corresponding SMD for the same computations as in Fig. 19. Consistent with the previous graph, we find that including shattering collisions lowers the mean drop size by a small amount, here about 20%, and the computation where we have restricted shattering to only collisions of $We > 1000$ lies about midway between the computation without

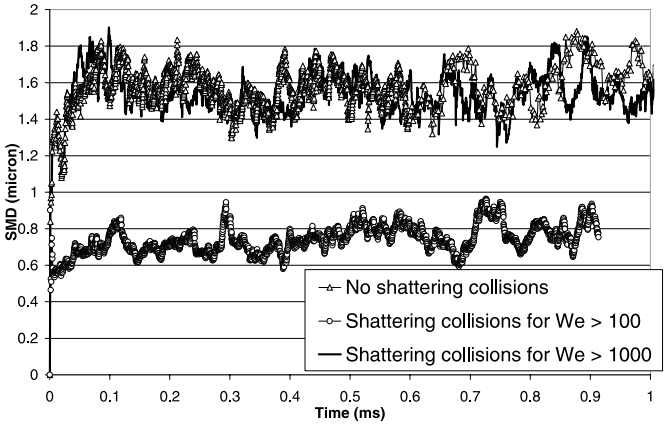

Fig. 21. Instantaneous SMD of drops in chamber for resolution of 220×110 cells.

shattering collisions and the one with shattering for $We > 100$. Fig. 21 shows the computed SMDs for the same three computations shown in Fig. 21, except that the high-resolution grid of 220 by 110 cells is used. Here the computations with no shattering collisions and shattering collisions for $We > 1000$ are very close together, while the computation with shattering collisions for $We > 100$ has a SMD that is about a factor of two lower. Shattering collisions may be important in a Diesel spray, but there is a need for considerable research in this area, especially in the possible affects of the ambient gas properties on shattering collisions. These computations, Figs. 16–21, in sprays show the interplay between effects of models and numerical resolution. If insufficient numerical resolution is employed, as is typical of diesel engine computations, the inadequacies in the numerics may dominate differences in models.

8. Summary and conclusions

Current models for the outcome of drop–drop collisions in Diesel sprays are based on the criterion proposed by Brazier-Smith et al. (1972) for water drops about 30 years ago. Recent measurements of drop-drop interactions indicate that there are significant differences in collision outcomes when hydrocarbon drops are employed. In this work, a composite model that accounts for the physics of hydrocarbon drops is implemented in a multidimensional model for Diesel sprays. The composite model accounts for bounce, grazing and reflexive separation and coalescence in drop–drop collisions. Effects of chamber density and shattering collisions are also included and shown to have an effect on the outcomes. It is shown that the composite model results in significantly lower coalescence rate compared to the Brazier-Smith et al. (1972) model. However, in the case of Diesel sprays, numerical inadequacies are more dominant than the inaccuracies associated with the collision/coalescence model.

There are several limitations of the composite model that have to be addressed. The experimental results on which the model is based have been carried out at pressures that are lower than 10 atm, whereas diesel injection is typically into an environment where the pressure is 50–100 atm. The effects of the differences in density on the outcomes of collisions may not be negligible as shown by Qian and Law (1997). We have proposed a model that includes the effects of density, but this model is derived from experimental data at 10 atm or less. Furthermore, the measurements are typically for equal-sized drops or drops that have a size ratio of 2. In Diesel sprays, the drop size ratios may be 10 or greater. The effect of these size ratios is not known. Additional studies of these parameters, and of effects of liquid properties apart from density and surface tension have yet to be carried out. Aerodynamic effects apart from bounce, effects of ambient vapor content and temperature are not considered. There is a need for considerable work in this area.

Acknowledgements

The authors acknowledge the support of the Army Research Office and Detroit Diesel Corporation for this work.

References

Aneja, R., Abraham, J., 1998. How far does the liquid penetrate in a diesel engine: computed results vs. measurements? Combustion Science and Technology 138, 233–256.

Ashgriz, N., Poo, J.Y., 1990. Coalescence and separation in binary collisions of liquid drops. Journal of Fluid Mechanics 221, 183–204.

Bracco, F., 1985. Modeling of engine sprays. SAE Transactions 94, 144–167.

Brazier-Smith, P., Jennings, S., Latham, J., 1972. The interaction of falling rain drops: coalescence. Proceedings of the Royal Society of London A 326, 393–408.

Chatwani, A., Bracco, F., 1985. Computation of dense spray jets. ICLASS 85, Paper 1B/1/1.

Estrade, J.P., Carentz, H., Lavergne, G., Biscos, Y., 1999. Experimental investigation of dynamic binary collision of ethanol droplets—a model for droplet coalescence and bouncing. International Journal of Heat and Fluid Flow 20, 486–491.

Frohn, A., Roth, N., 2000. Dynamics of Droplets. Springer, New York.

Gavaises, M., Theodorakakos, A., Bergeles, G., Breen, G., 1996. Evaluation of the effect of droplet collisions on spray mixing. Proceedings of the Institution of Mechanical Engineers 210, 465–475.

Georjon, T.L., Reitz, R.D., 1999. Drop-shattering collision model for multidimensional spray computations. Atomization and Sprays 9, 231–254.

Gosman, A., Ioannides, E., 1981. Aspects of Computer Simulation of Liquid-Fueled Combustors. AIAA Paper 810323.

Gunn, R., 1965. Collision characteristics of freely falling water drops. Science 150, 695–701.

Jiang, Y., Umemura, A., Law, C.K., 1992. An experimental investigation on the collision behaviour of hydrocarbon droplets. Journal of Fluid Mechanics 234, 171–190.

Magi, V., 1987. REC-87: A new a3-D code for flows, sprays, and combustion in reciprocating and rotary engines. Mechanical and Aerospace Engineering Report no. 1793, Princeton University.

Magi, V., 1999. REC-2000: A multidimensional code for transient, two-phase, turbulent reacting flows. Engine Research Laboratory Report, School of Mechanical Engineering, Purdue University.

Menchaca-Rocha, A., Huidobro, F., Martinez-Davalos, A., Michelian, K., Perez, A., Rodriguez, V., Carjan, N., 1997. Coalescence and fragmentation of colliding mercury drops. Journal of Fluid Mechanics 346, 291–318.

O'Rourke, P., Bracco, F., 1980. Modeling of drop interactions in thick sprays and a comparison with experiments. Proceedings of the Institution of Mechanical Engineers 9, 101–106.

Orme, M.E., 1997. Experiments on droplet collisions, bounce, coalescence and disruption. Progress in Energy Combustion Science 23, 65–79.

Park, R.W., 1970. Behavior of water drops colliding in humid nitrogen. Ph.D. Dissertation, University of Wisconsin, Madison.

Qian, J., Law, C.K., 1997. Regimes of coalescence and separation in droplet collision. Journal of Fluid Mechanics 331, 59–80.

Reitz, R.D., Diwaker, R., 1987. Structure of high-pressure fuel sprays. SAE Paper 870598.

Siebers, D.L., 1998. Liquid-phase fuel penetration in Diesel sprays. SAE Paper 980809.

Tennison, P.J., Georjon, T.L., Farrell, P.V., Reitz, R.D., 1998. Experimental and numerical study of sprays from a common rail injection system for use in an HSDI diesel engine. SAE Paper 980810.

Willis, K.D., Orme, M.E., 2000. Experiments on the dynamics of droplet collisions in a vacuum. Experiments in Fluids 29, 347–358.